

Cast titanium as implant material

S. MOHAMMADI¹, L. WICTORIN², L. E. ERICSON¹, P. THOMSEN¹

¹*Department of Anatomy and Cell Biology, University of Göteborg, Sweden*

²*Structural Biomaterials, Institute of Surface Chemistry, Stockholm, Sweden*

The tissue response in rats to implants made of machined and cast titanium was evaluated after 1 and 12 weeks. The implants consisted of a circular plate portion, located in the abdominal wall, and a cylindrical rod portion protruding into the peritoneal cavity. The chemical and topographical surface properties of the two types of implants differed considerably. The implants with surrounding tissue were processed en bloc for light and electron microscopy. The bulk metal was removed by an electrochemical procedure which permitted the sectioning and evaluation of the intact implant–tissue interface. The general distribution of macrophages and fibroblasts was the same around the plate portion of both types of implants. Macrophages constituted the predominating cell type with the highest concentration in the innermost cell zone closest to the implant. The number of macrophages per section area was significantly higher around machined implants. Multinuclear giant cells, always located at the implant surface, were more frequent around cast implants. The majority of the intraperitoneal rod portions were partially (1 week) or completely (12 weeks) covered by tissue; partial or complete overgrowth of tissue was rare for machined rod portions. Imaging electron energy loss spectroscopy demonstrated the presence of titanium in macrophages in the peripheral part of the tissue capsule around cast, but not machined implants. We conclude that the tissue responses to the two types of titanium implants differed considerably in the two biological environments (soft tissue in abdominal wall; peritoneal cavity) examined and that the response in one environment does not predict the response in the other. We also believe that improvements have to be made in the casting procedure in order to reduce surface roughness and contamination before cast implants can be used in clinical applications.

1. Introduction

Titanium (Ti) implants, usually manufactured by machining, are used in various clinical applications, most notably as intraosseous implants in the oral and craniofacial region [1]. Experimental and clinical studies have shown that implants of non-alloyed Ti have a favourable biological performance in soft tissue as well as in bone [2, 3]. During optimal conditions a direct contact is established between the implant and bone without any intervening fibrous tissue, a situation often referred to as osseointegration [1]. This intimate bone–implant contact promotes mechanical stability and is most likely a major reason for the good clinical long-term results obtained. However, due to its mechanical properties, Ti is less suitable for implants carrying heavy loads, as for instance hip joint prostheses. In such applications titanium alloys (Ti6Al4V) are used. A potential disadvantage with this alloy is the possibility of leakage of aluminum and vanadium [4] with potential toxic effects on the surrounding tissue.

During recent years cast titanium has attracted an increasing interest in the biomedical area, mainly in

restorative dentistry. For various devices casting of titanium may have advantages from manufacturing, mechanical and economical points of view [5, 6]. The use of cast titanium in biomedical applications has been restrained by the difficulties in overcoming inherent casting problems. Titanium has a high melting point and molten titanium is extremely reactive with elements such as nitrogen and oxygen as well as with elements in the casting investment [7–9], resulting in poor surface quality and dimensional inaccuracies [8, 10]. Provided the casting process is modified and more accurately controlled [9], the casting technique may have applications also in the production of biomedical implants. At present nothing is known about the biological performance of cast titanium. In the present study we have therefore compared the tissue response to implants of machined pure titanium and cast titanium. The design of the implants, with a part in contact with the soft tissue in the rat abdominal wall and another part protruding into the peritoneal cavity, permitted the evaluation of the biological response in two different biological environments. The study also included a preliminary

examination of the chemical composition of cast titanium.

2. Materials and methods

2.1. Implants

Cast and machined implants had the same shapes and dimensions and consisted of a circular plate (thickness 0.5 mm; diameter 4 mm) to which a cylindrical rod (length 3 mm; diameter 2 mm) was attached [11].

Large irregularities of the cast implants were removed by sandblasting and mechanical treatment with sandpaper discs followed by washing in ethanol. Before implantation, cast and machined implants were cleaned ultrasonically in baths of trichlorethylene and ethanol and sterilized by autoclaving.

2.2. Casting procedure

Implants were cast from wrought Ti rods (grade II; JMI-125 from JMI-Ti Ltd; diameter 21 mm). Casting was performed in an equipment designed for dental castings (Castmatic, Iwaton Co., Osaka, Japan). The Ti was melted by an arc heating system in an argon atmosphere, essentially according to a previously described procedure [9]. The mould was made of Rema Titan (Dentanrum, Chemie Labor, Germany). The mould material was mixed with water and treated according to the recommendations given by the manufacturer.

2.3. Metallographic studies

Cast titanium was analysed in a Jeol JSM-840 scanning electron microscope (SEM) equipped for X-ray elemental analysis (Link AN-10000 unit). Cast specimens, treated with sandblasting, sandpapering and cleaning as described above, were embedded in plastic. A plane surface perpendicular to the surface of the plate portion was produced by grinding. The ground surface was then etched by treatment with hydrofluoric acid before elemental analysis. The surface topography of cast and machined implants was examined by scanning electron microscopy (secondary electron mode) using a Jeol JSM T-300.

2.4. Animals and anaesthesia

Adult Sprague-Dawley male rats (Alab, Södertälje, Sweden) weighing 250–300 g and fed on a standard pellet diet and water *ad libitum* were used. The rats were anaesthetized by an intraperitoneal injection of a mixture of nembutal (60 mg/ml), diazepam (5 mg/ml) and saline in 1:2:1 volume proportions. Ten rats were used in each group. Some tissue specimens were excluded from further evaluation due to poor quality of tissue preservation. The experiments were approved by the Gothenburg Local Ethical Animal Experiments Committee.

Machined and cast Ti implants were inserted in the abdominal wall of rats using a procedure previously

described in detail [12]. Each rat received two implants, one of each kind, placed 10 mm apart immediately to the right part of the linea alba of the abdominal wall. The rod portion penetrated through the peritoneal membrane into the abdominal cavity while the circular plate was located inside the abdominal wall in contact with the rectus abdominis muscle [12].

2.5. Tissue preparation

The follow-up periods were 1 and 12 weeks. The rats were anaesthetized and then fixed by perfusion via the left heart ventricle with 2.5% glutaraldehyde in 0.05 M sodium cacodylate, pH 7.4. The implants were excised together with the surrounding abdominal wall. The peritoneal surface with the implant rod portion was photographed in a stereomicroscope in order to document the amount of tissue covering the rod. The implants with surrounding tissue were left in glutaraldehyde overnight and then postfixed in 2% OsO₄ for 1 h. The samples were then dehydrated in ethanol and finally embedded in epoxy resin (Agar 100, Agar Aids, Stansted, Essex, England).

The bulk metal in the embedded specimens was removed by an electrochemical dissolution technique. In this procedure the surface oxide layer is not removed and the intact implant-tissue interface can be sectioned [13].

Light microscopic (LM) sections (1 µm thick) were cut on an ultramicrotome using glass knives and stained with Azur II and 0.5% methylene blue in 1% disodium tetraborate. Ultrathin sections, cut with a diamond knife from areas selected in the LM, were stained with uranyl acetate and lead citrate before examination with transmission electron microscopy, using a Philips EM 400 or a Zeiss EM 902, the latter equipped with an electron energy loss spectrometer (EELS) used to study the distribution of Ti in the tissue.

2.6. Morphometry

Semi-thin sections were analysed essentially according to Röstlund *et al.* [14] using a Nikon Microphot-FXA light microscope with a 40× objective and a 10× eyepiece fitted with a square grid. LM morphometry, in one section for each implant, was performed on the tissue located at the surface of the plate portion facing the abdominal cavity. A dense line, representing the metal oxide surface remaining after the electrochemical removal of the bulk metal (and thus the implant surface) could be observed in the sections. The width of the space (fluid space) present after 1 week between this line and the organized tissue was determined. In specimens retrieved after 12 weeks (when the fluid space was absent) the width of the organized connective tissue (capsule) was measured (mean of five points for each implant). Evaluation of cell distribution was performed in five different regions along the interface. The first region was located 200 µm from the lateral border of the implant and the remaining four regions

were located consecutively, separated by a distance of 120 μm , along the interface. In each region the tissue outside the implant was divided into four zones, each 20 μm in depth and 80 μm in width with zone 1 located adjacent to the fluid space (1 week) or implant surface (12 weeks). In each zone the number of monocytes/macrophages and fibroblasts was determined. The number of other cell types (together about 10% of all cells), including non-identified cells (about 3%), was also determined (data not presented).

The mean values for each zone obtained in the five regions in each section were calculated. The mean values for each group of animals were then calculated (1 week: machined titanium $n = 10$, cast titanium $n = 8$; 12 weeks: machined titanium $n = 9$, cast titanium $n = 8$). The data were evaluated statistically using a generalized linear model (GLM).

3. Results

3.1. Surface morphology of implants

In the scanning electron microscope the surface of the cast implants (Fig. 1a, b) had a very irregular surface characterized by elevations and depressions of varying shapes and dimensions. The machined Ti implants were characterized by the presence of typical, parallel

machining ridges and grooves which were 2–5 μm in width. Elevations and pits were superimposed on this pattern (Fig. 2a, b).

3.1.1. Metallographical analysis

As a back-ground for the biological studies a preliminary elemental analysis was performed using X-ray analysis (Fig. 4).

Only a few porosities or cracks could be observed in the implant surface. In a few areas particles of the investment material remained located in a surface defect. An example of this is shown in Fig. 3. Investment material not related to surface defects was probably removed by the sandblasting and sandpapering procedures used.

As illustrated in Figs 3 and 4 the surface portion of the implant consisted of three layers. The outer reaction layer (labelled 1 in Fig. 3) consisted of investment material incorporated in the Ti melt. Ti, P, O, Al, Mg and Si were found in this layer. The inner reaction layer (labelled 2 in Fig. 3) contained, besides Ti, dissolved P, O, Al and Si. This layer has previously been described [9], due to its crystal organization, as the alfa-case. A third layer (labelled 3 in Fig. 3) was sharply demarcated from the inner reaction layer and

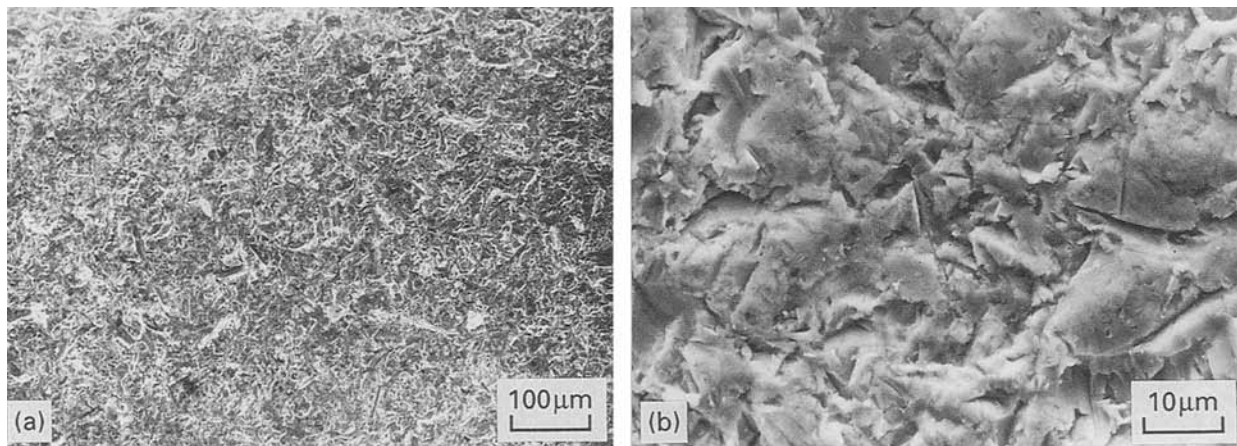


Figure 1 (a, b) Scanning electron micrographs of the surface of cast Ti implants. The surface topography is very irregular.

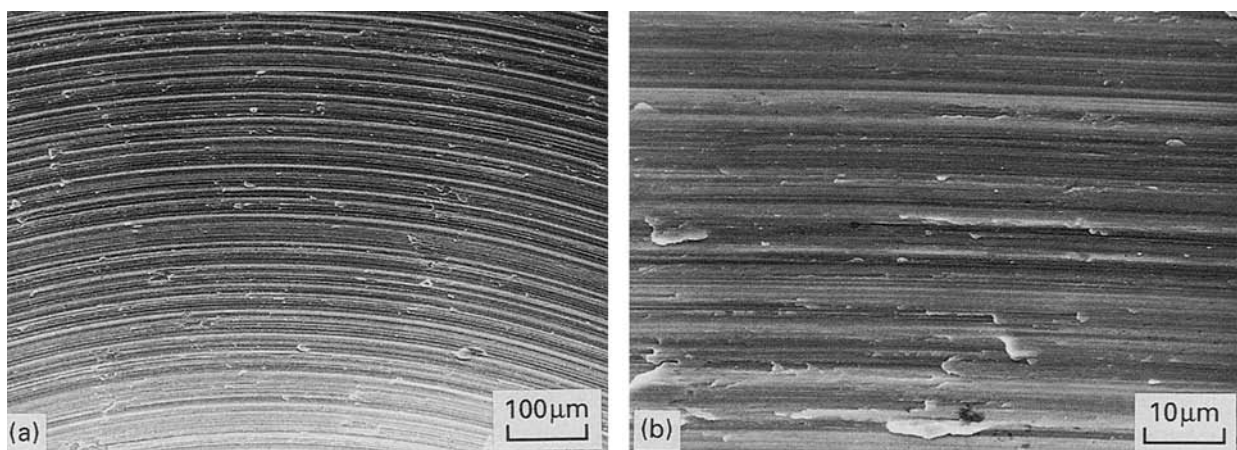


Figure 2 (a, b) Scanning electron micrographs of the surface of machined Ti implants. The surface topography is characterized by parallel grooves.

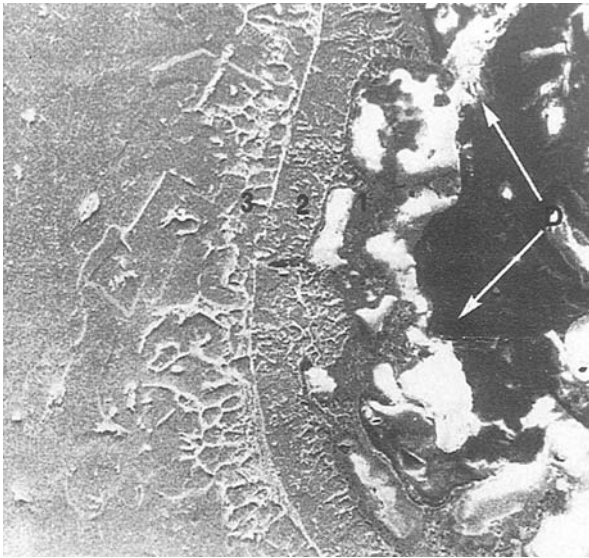


Figure 3 Scanning electron micrograph of the ground surface of a cast Ti implant. The implant surface with a defect (D) containing material derived from the investment material. Outer (1) and inner (2) reaction layers as well as a third (3) layer gradually intermingling with the implant core can be distinguished. Magnification $\times 1000$.

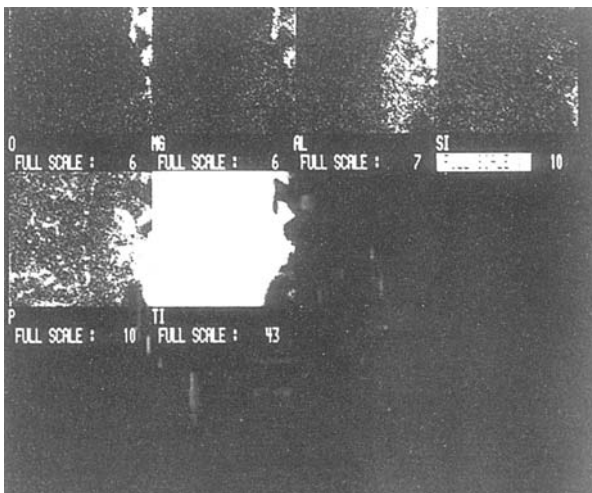


Figure 4 Elemental mapping using X-ray analysis in the scanning electron microscope at the outer reaction layer. Besides Ti, P is the dominating element, but other elements (Al, Si, Mg and O) are also present. Magnification $\times 950$.

intermingled centrally gradually with the melt proper without any distinct demarcation. This layer was, in the scanning electron microscope, characterized by dark areas separated by narrow, bright lines. Ti, P and O were present in this layer.

3.2. Tissue organization and morphometry

A clear difference was found between cast and machined Ti implants with respect to the tissue reaction towards the intraperitoneal rod portion (Fig. 5). The majority of cast specimens (5/8 specimens) were, at 1 week, covered by tissue on at least half of the rod portion protruding into the abdominal cavity. Growth of tissue on the rod portion was more rarely

seen around rods of machined implants (1/10 specimens at 1 week; 1/9 at 12 weeks); at 12 weeks the majority of intraperitoneal rod portions of cast implants were completely covered by tissue (6/8 specimens).

In sections of the tissue around the plate portion retrieved after 1 week a fluid space was present between the implant surface, marked by the remaining surface oxide appearing as a thin dark line in sections, and the surrounding tissue (Fig. 6). The fluid space contained scattered inflammatory cells, predominantly monocytes/macrophages and in some specimens also scattered red blood cells. The width of the fluid space varied within the same section as well as between sections of different specimens. One week after surgery, the mean widths of the fluid space around machined Ti ($19 \mu\text{m} \pm 6.3 \mu\text{m}$; mean \pm standard error of the mean, SEM) and cast Ti ($14 \mu\text{m} \pm 3.7 \mu\text{m}$; mean \pm SEM) implants were not significantly different. At 12 weeks the tissue was very close to the surface and no fluid space could be distinguished (Fig. 7).

The general organization of the tissue after 1 and 12 weeks was the same for both types of implants. At 1 week the newly formed tissue around the implants did not have any distinct outer limit, making measurements of capsule width uncertain. After 12 weeks the capsule was sharply demarcated from the surrounding loose connective tissue. The capsule thicknesses (machined Ti: $111 \mu\text{m} \pm 10 \mu\text{m}$; mean \pm SEM; cast Ti: $90 \mu\text{m} \pm 13 \mu\text{m}$; mean \pm SEM) were not significantly different.

After 12 weeks the innermost portion of the capsule consisted of one to four layers of predominantly macrophages but also fibroblasts. A multilayered fibrous tissue consisting of fibroblasts and macrophages separated by collagenous bundles was located peripheral to the implant-close cell layers. In the tissue surrounding the cast Ti implants a conspicuous feature was the presence of large macrophages with dense particles in their cytoplasm. These macrophages were located in association with the blood vessels peripheral to the fibrous layer and were not observed in locations closer to the implants (Fig. 7a). As further described below these macrophages contained Ti.

Macrophages were the most common cells in all four zones around both types of implants and at both time intervals (Fig. 8). A significantly higher concentration ($p < 0.01$) of macrophages was found around machined Ti implants after 12 weeks. As shown in Fig. 8 the highest concentration was found in zone 1, closest to the implant surface. Multinuclear giant cells, always located at the implant surface, were mainly present around cast Ti implants after 12 weeks and were about six times more frequent than around Ti implants (Fig. 10). At both time intervals the concentration of fibroblasts around machined implants tended to be higher in all zones but the difference between the two types of implants was not statistically significant (Fig. 9). Focal accumulations of lymphocytes were also present around both types of implants, mainly in relation to blood vessels in zones 2 and 3. These cells appeared, after 1 week, around both

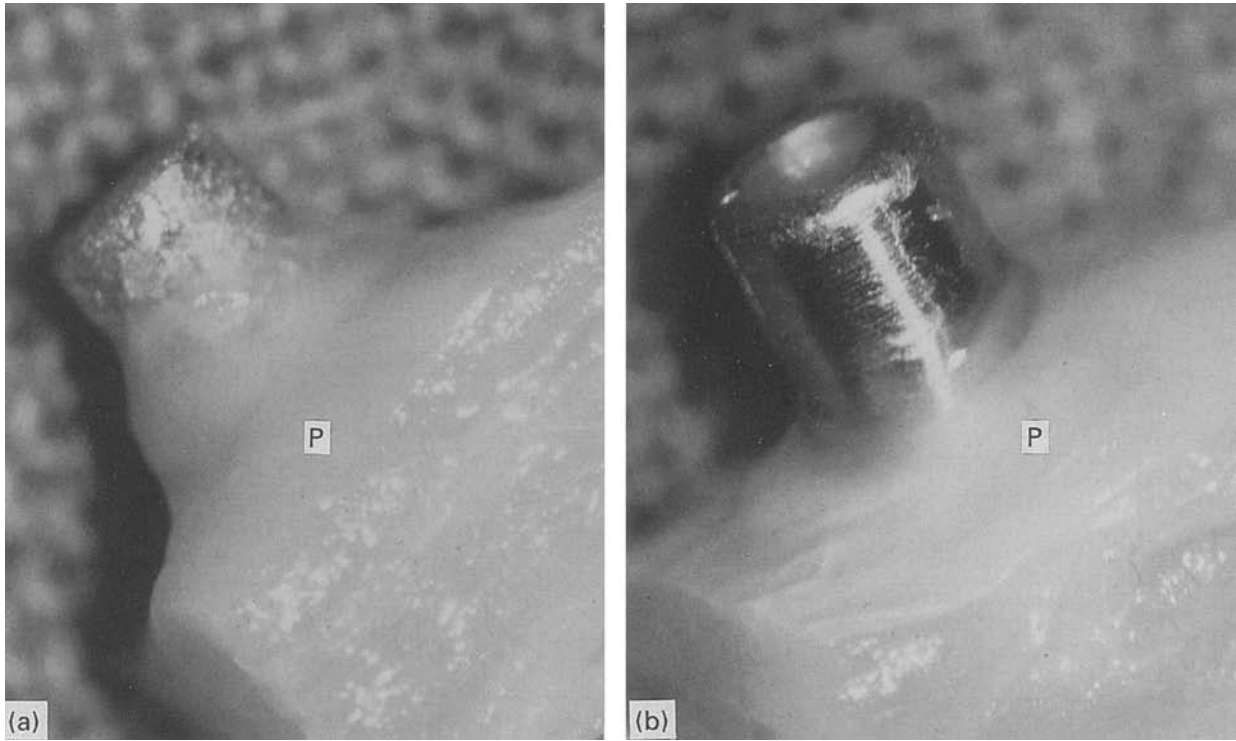


Figure 5 Photographs of rod portion of cast (a) and machined (b) Ti implants 1 week after implantation. The rod portion penetrates the peritoneal membrane (P) and protrudes into the abdominal cavity. The cast Ti implant has an irregular surface and is partly covered by tissue (after 12 weeks the entire rod was, in general, covered by tissue). No tissue overgrowth can be seen on the rod of the machined implant (b).

materials. However, in comparison to fibroblasts and macrophages the number of lymphocytes was low. In addition, mast cells and eosinophilic leukocytes were regularly found in all zones after 12 weeks.

3.3.1. Ultrastructure

In the electron microscope, attention was mainly focused on the organization of cells located close to the implant surface, that is within zone 1. The surface of the electropolished machined Ti implant (visible as a dark line in light microscopy and transmission electron microscopy and representing the oxide surface [13]) had a smooth outline with a rather constant (8–12 nm) width (Fig. 11). In contrast, the dark line of the cast implants was very irregular and had a varying thickness (Fig. 11). This thick surface layer often resulted in poor section quality. As described above, the 1 week implants were surrounded by a fluid space containing proteinaceous material and scattered inflammatory cells, predominantly monocytes/macrophages, only a few of which were attached to the implant surface. The border of the tissue towards the fluid space was formed by distinct strands of fibrins to which macrophages, most often elongated with cytoplasmic extensions, were adhering. Thus, fibrin was present in this region rather than associated with the implant surface, which is in accordance with our previous immunohistochemical findings [15].

After 12 weeks the fluid space was, in general, absent and cells (macrophages and multinuclear giant cells) had established contact with the implant surface (Fig. 7). The predominant cell type in contact with the implant surface was macrophages. Most macrophages

at the implant surface were closely attached, with a plasma membrane adapting to the surface (Ti) also when this was very irregular as for cast implants (Fig. 11). Collagen was not found in this innermost cell zone.

The multilayered fibrous capsule consisted of flat fibroblasts, and also macrophages of similar shape, separated by collagen bundles. As observed in the light microscope, in tissue surrounding cast implants macrophages containing dense particles were located in the loose connective tissue peripheral to the multilayered fibrous tissue in association with blood vessels (Fig. 7a). In the electron microscope these macrophages had numerous phagocytic vacuoles (Fig. 12). Using imaging EELS, Ti was identified in the vacuoles. Ti appeared both in dense, angular fragments as well as in a finely granular material (Fig. 13). Ti was not found in any location closer to the implants.

4. Discussion

In the present study Ti implants were cast using Rema Titan as the investment material. Compared to five other investment materials previously examined [9], Rema Titan appeared to induce fewer porosities and more limited reaction layers in the casting. However, to fully evaluate Rema Titan, additional, quantitative documentation is required.

Molten Ti reacts with the mould material resulting in the formation of surface reaction layers which, besides Ti, contain elements from the mould [7,9]. The dimensions and composition of these reaction layers are dependent on several factors such as the

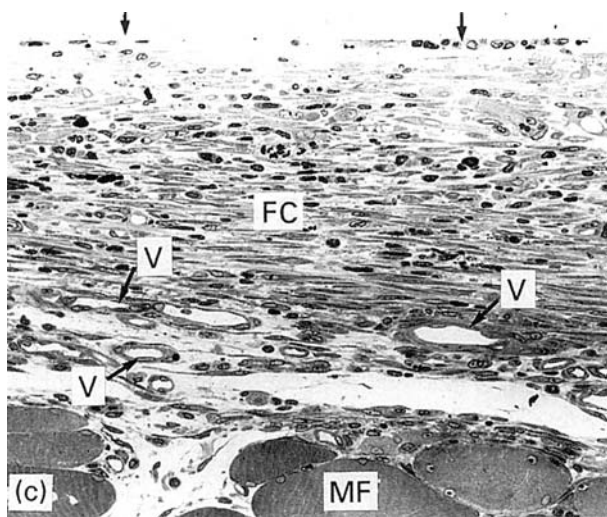
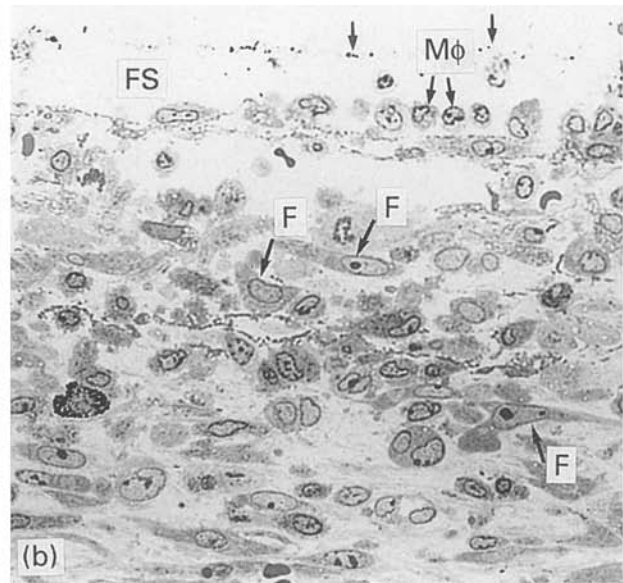
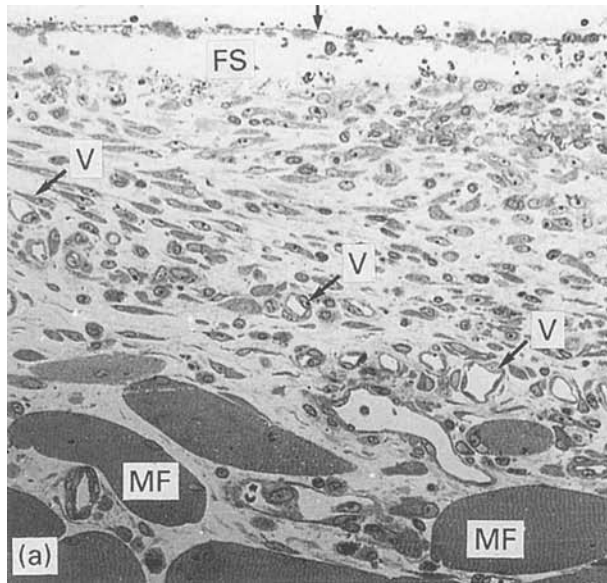


Figure 6 Light micrographs of the tissue adjacent to implants retrieved from the abdominal wall after 1 week. The bulk metal was removed electrochemically to allow sectioning of the intact interface (a) Cast Ti implant. The implant surface is seen as a rather irregular line (arrows). The tissue is separated from the implant by a fluid space (FS). The tissue is loosely arranged and a fibrous capsule cannot be distinguished. Newly formed vessels (V) are located in the peripheral portion of the tissue adjacent to muscle fibres (MF). Magnification $\times 290$. (b) Cast Ti implant. Implant surface is marked by arrows. The tissue is separated from the implant by a fluid space (FS). Some macrophages (M ϕ) and fibroblasts (F) in the tissue are indicated. Magnification $\times 570$. (c) Machined Ti implant. The implant surface (arrows) is smooth. The tissue has started to organize in a fibrous capsule (FC) with elongated profiles of macrophages and fibroblasts. V = blood vessels MF = muscle fibres. Magnification $\times 245$.

investment material, mould temperature and atmosphere in the casting equipment [9]. We used X-ray analysis to analyse the element composition of the reaction layers and found that, besides Ti, P and O were predominant but also that a number of other elements were present. Although a major portion of the outer reaction layer probably was removed before implantation, it is obvious that the surface chemistry of cast Ti implants differs considerably from that of machined implants. In the latter the main surface component is TiO₂ although small amounts of contaminants, mainly carbon, also are present [16]. The cast implants had a very irregular surface topography which was quite different from that of the machined implants. Thus, the two types of implants had different chemical as well as topographical surface properties. This difference was also evident in the specimens examined by TEM in which the bulk metal was removed by electropolishing. In specimens of machined implants the dense line, representing the surface titanium dioxide [13], was thin and had an even thickness; in cast specimens the material remaining after electrochemical treatment had an uneven thickness and a very irregular outline.

In the morphometric evaluation the general distribution of macrophages and fibroblasts, the predominant cell types around the two types of implants, were essentially the same. One difference, however, was the large number of multinuclear giant cells found in contact with the surface of cast implants. Previous studies [3, 17–21] indicate that the appearance of multinuclear giant cells is influenced by the surface roughness, suggesting the possibility that the increased number of multinuclear giant cells is related to the irregular surface topography of these implants. However, the increased number of multinuclear giant cells was not accompanied by an increased thickness of the reactive tissue capsule. On the contrary, the concentration of cells around cast implants was lower. In the innermost zone (zone 1) this was partly explained by the fact that macrophages were replaced by multinuclear giant cells, but we have no explanation for the lower cell densities found also in other zones of the capsule.

The experimental method used allows the biological reaction to an implant to be simultaneously examined in two different biological environments: the abdominal wall and the peritoneal cavity. In the present

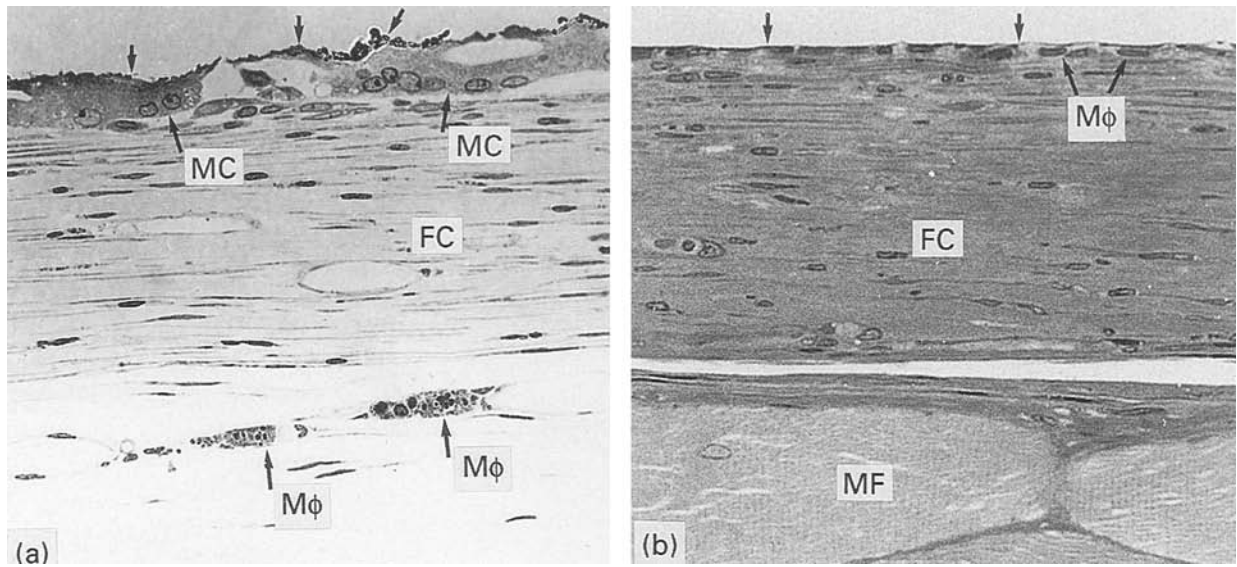


Figure 7 Tissue adjacent to implants retrieved after 12 weeks. Specimens were treated electrochemically. At this time interval the fluid space has disappeared. (a) Cast Ti implant. The implant surface (arrows) is marked by a thick, irregular dense line. Multinuclear giant cells (MC) are located in contact with the surface. A fibrous capsule (FC) consisting of collagen and elongated cell profiles is present. Large macrophages (M ϕ) containing dense material are located peripheral to the capsule. Magnification $\times 490$. (b) Machined Ti implant. The implant surface (arrows) has a smooth outline and is separated from the fibrous capsule (FC) by two or three layers of macrophages (M ϕ). MF = muscle fibres. Magnification $\times 480$.

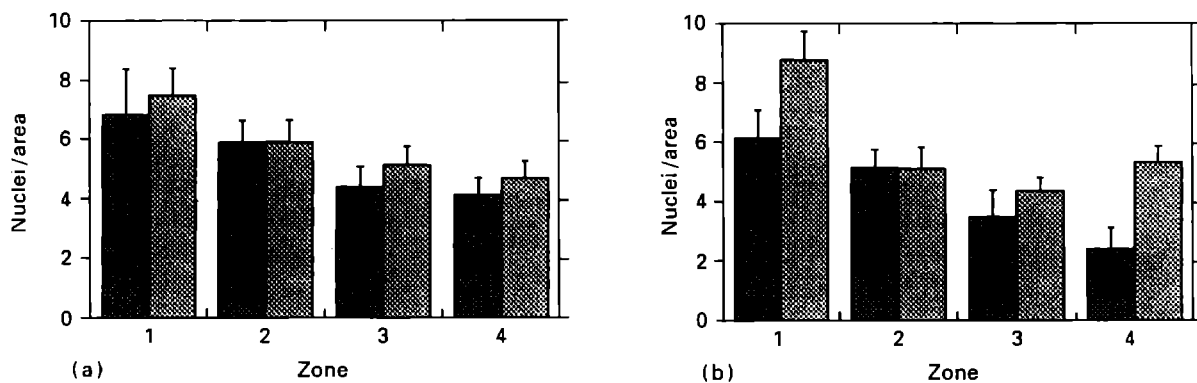


Figure 8 Light microscopic morphometry. Distribution of macrophages in zones 1–4 (see Section 2). Nuclear profiles/1600 μ^2 , Mean \pm SEM. The distribution of macrophages is similar for the two types of implants after 1 week (a). After 12 weeks (b) significantly more macrophages ($p < 0.01$) are present around machined Ti implants, mainly in zones 1 and 4. (■ cast; ▨ machined)

study we found that the intraperitoneal rod portion of the majority of cast Ti implants were covered by tissue both 1 and 12 weeks after implantation, while the great majority of machined Ti implants were free of tissue. In conjunction with the observations on the tissue reaction in the abdominal wall this emphasizes the point that the biological reactions to a biomaterial can be quite different in different biological environments and that information concerning the biological performance of a biomaterial in a particular tissue environment is not applicable to other tissues. We recently made similar observations for silicone implants, which induced a tissue reaction in the abdominal wall similar to that of machined Ti implants. In contrast, the intraperitoneal portion of silicone implants was covered by tissue whereas most of the Ti implants, as found in the present study, were free of enveloping tissue [22].

Ti identified by imaging EELS was found in phagocytic vacuoles in macrophages located in the tissue surrounding cast (but not machined) implants. This does not appear as an astonishing finding considering the structure of the surface structure of the cast implants. An interesting observation is that the Ti-containing macrophages invariably were located adjacent to vessels in the peripheral portion of the capsule, and never close to the implant surface. A similar peripheral location of Ti-containing macrophages has also been found in the tissue surrounding Ti implants covered by a Ti-peroxy gel [2]. The mechanism leading to the accumulation of these macrophages to a restricted peripheral zone in the capsule is unknown but may be related to the presence of numerous vessels, largely absent from the inner zones of the capsule, in this location.

The present study shows that cast and machined Ti implants of identical shape and dimensions but with

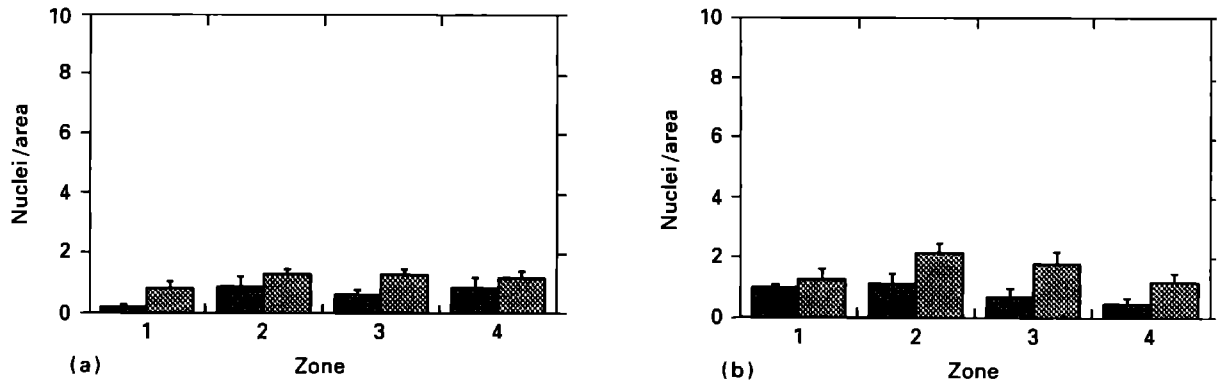


Figure 9 Light microscopic morphometry. Distribution of fibroblasts. Although a higher cell density is found around machined implants there is no statistical difference between the two types of implants (a) 1 week; (b) 12 weeks (■ cast; ▨ machined).

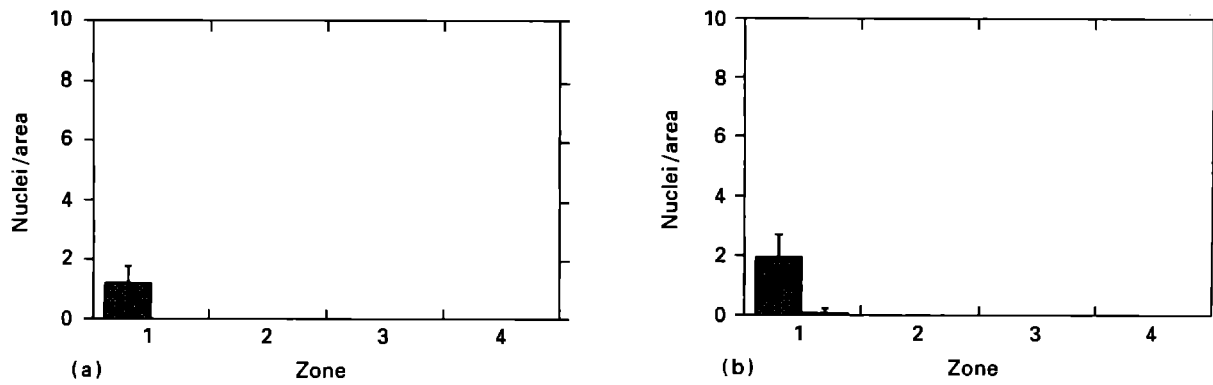


Figure 10 Distribution of multinuclear giant cells. These cells are only detected in zone 1, close to the implant surface and mainly in specimens with cast Ti implants: (a) 1 week; (b) 12 weeks (■ cast; ▨ machined).

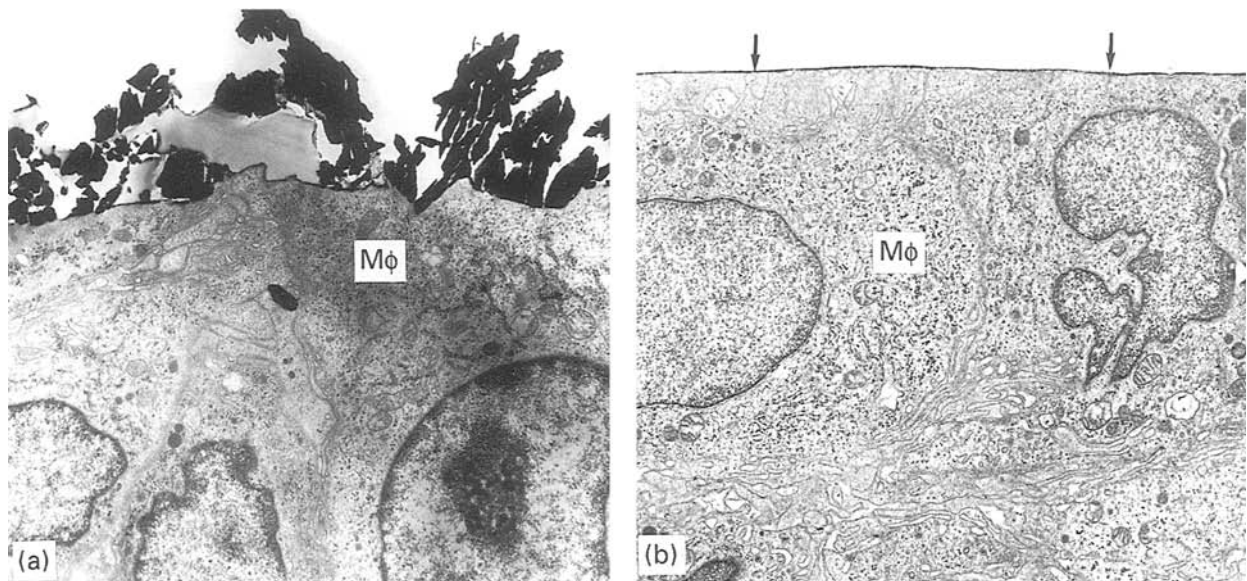


Figure 11 Implants retrieved from abdominal wall after 12 weeks. The specimens were treated electrochemically in order to remove the bulk metal. (a) Cast titanium implant. Fragments of titanium, and possibly also of other components derived from the investment material, remain. Macrophages (Mφ) are in contact with the irregular implant surface. Magnification × 5000. (b) Machined implant. The surface oxide layer remaining after the electrochemical treatment forms a thin, smooth line representing the implant surface. Macrophages (Mφ) are in contact with the implant surface. Magnification × 5000.

widely different surface properties elicit different biological responses both in the abdominal wall and in the peritoneal cavity. The significance of the reduced concentration of fibroblast and macrophages

found around cast Ti implants is uncertain. Our findings point to the problem of interpretation of morphometric information in biomaterials studies and indicate that other methods, evaluating for

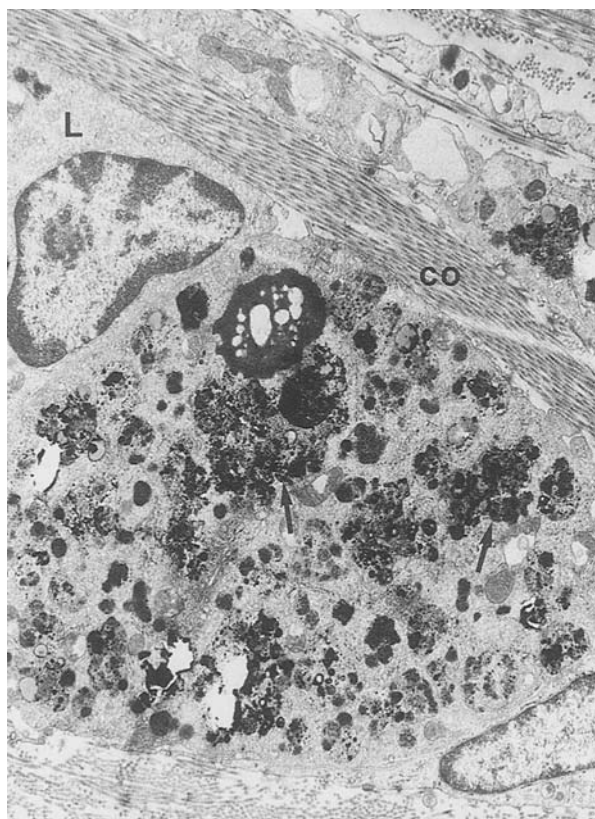


Figure 12 Cast titanium implant, 12 weeks. A macrophage is located peripheral to the fibrous capsule and contains numerous phagocytic vacuoles (some of which are indicated by arrows) filled with dense material. L = lymphocyte. Co = collagen. Magnification $\times 6500$.

instance various aspects of cell activity and composition of the extracellular matrix, should be considered as a complement to quantitative evaluations of the cells surrounding implants. The increased number of

multinuclear giant cells at the surface of cast Ti implants was not related to an increased thickness of the capsule in this short-term study but their presence might be of importance in a long-term perspective. However, a general impression is that pronounced differences in topographical and chemical surface properties corresponded to only minor differences in the overall tissue response in the abdominal wall. An interpretation of this is that other factors than the physicochemical properties of the implant, for instance degree of tissue trauma or movements of tissues, are equally or more important for the tissue response and organization of the tissue. The interaction between the peritoneal fluid and the implant may, at least in an initial phase, have similarities to the blood-biomaterials interaction and in this situation the surface properties may have a relatively more important role than in an organized tissue. This could explain the early and clear differences found for intra-abdominal reaction to cast and machined Ti implants.

From the present study it is not possible to draw any definite conclusions concerning the suitability of cast titanium as an implant material. It should be pointed out that in this study the casts underwent only a brief polishing procedure before insertion, which only slightly modified the surface. Cast implants should probably be treated by procedures aimed at a reduction of surface roughness and removal of mould contaminants from the surface.

Acknowledgements

The authors would like to thank Mrs Lena Emanuelsson and Mrs Gunnel Bokhede for their skilful technical assistance and Lotta Hallberg for help with the statistical evaluation. This study was supported by the Inga-Britt and Arne Lundberg's Science Foundation,

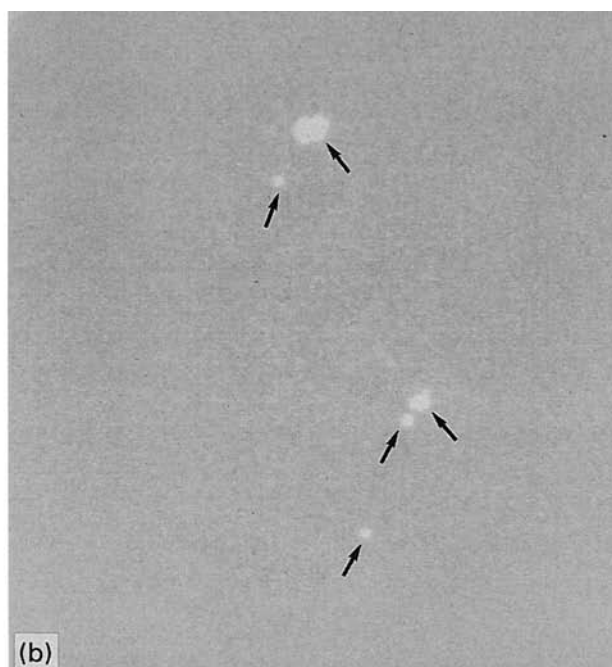
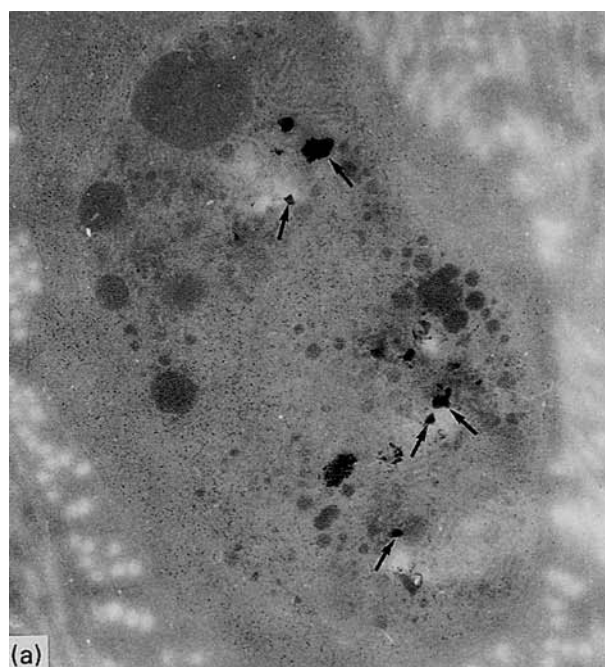


Figure 13 Imaging electron energy loss spectroscopy (EELS) of titanium. A macrophage located peripheral to the fibrous capsule. The uncontrasted cell profile is shown in (a) and the element distribution picture in the same profile (b). Arrows indicate corresponding points in the two micrographs. Magnification $\times 34000$.

the King Gustav V 80-year Fund, the Swedish National Association Against Rheumatism, The Faculties of Medicine and Odontology, University of Gothenburg, The Swedish National Board for Technical Development (NUTEK) and The Swedish Medical Research Council (9289 and 9495).

References

1. R. ADELL, B. ERICSSON, U. LEKHOLM, P. I. BRÅNEMARK and T. JEMT, *Int. J. Oral. Maxillofacial implants* **5** (1990) 347.
2. L. E. ERICSON, B. R. JOHANSSON, A. ROSENGREN, L. SENNERBY and P. THOMSEN, in "The bone-biomaterial interface", edited by J DAVIS (Toronto University Press, 1991) p. 425.
3. P. THOMSEN and L. E. ERICSON, in "The bone-biomaterial interfaces", edited by J. DAVIES (Toronto University Press, 1991) p. 153.
4. C. B. JOHANSSON, T. ALBREKTSSON, P. THOMSEN, L. SENNERBY, A. LODDING and H. ODELIUS, *Eur. J. Exp. Musculoskel. Res.* **1** (1992) 161.
5. H. HAMANAKA, H. DOI, T. YONEYAMA and O. OKUNO, *J. Dent. Res.* **68** (1989) 1529.
6. M. TAIRA, J. B. MOSER and E. H. GREENER, *Dent. Mater. J.* **5** (1989) 45.
7. O. MIYAKAWA, K. WATANABE, S. OKAWA, S. NAKANO, M. KOBAYASHI and N. SHIOKAWA, *ibid.* **8** (1989) 175.
8. J. TAKAHASHI, H. KIMURA, E. P. LAUTENSCHLAGER, J. H. CHERN LIN, J. B. MOSER and E. H. GREENER, *J. Dent. Res.* **69** (1990) 1800.
9. L. WICTORIN, N. EI. MAHALLAWY, M. A. TAHA and H. FREDRIKSSON, *Cast Metals* **4** (1992) 182.
10. R. BLACKMAN, N. BARGHI and C. TRAN, *J. Pros. Dent.* **65** (1991) 309.
11. P. THOMSEN and L. E. ERICSON, *Biomaterials* **6** (1985) 421.
12. P. THOMSEN, L. M. BJURSTEN and L. E. ERICSON, *Scand. J. Plast. Reconstr. Surg.* **20** (1986) 173.
13. L. M. BJURSTEN, L. EMANUELSSON, L. E. ERICSON, P. THOMSEN, J. LAUSMAA, L. MATTSSON, U. ROLANDER and B. KASEMO, *Biomaterials* **11** (1990) 596.
14. T. RÖSTLUND, P. THOMSEN, L. M. BJURSTEN and L. E. ERICSON, *J. Biomed. Mater. Res.* **24** (1990) 847.
15. A. ROSENGREN, B. R. JOHANSSON, P. THOMSEN and L. E. ERICSON, *Biomaterials* **15** (1994) 17.
16. J. LAUSMAA and L. LINDER, *ibid.* **9** (1988) 277.
17. K. SMETANA, Jr., J. VACIK, D. SOUCKOVA, Z. KRKOVA and J. SULC, *J. Biomed. Mater. Res.* **24** (1990) 463.
18. S. B. GOODMAN, V. L. FORNASIER, J. LEE and J. KEI, *ibid.* **24** (1990) 517.
19. M. AMON and R. MENAPACE, *J. Cataract Refract. Surg.* **17** (1991) 774.
20. K. UENOYAMA, M. TAMURA, C. KINOSHITA, R. KANAGAWA, S. OHMI, T. NAKAO and S. SAIKA, *ibid.* **16** (1990) 465.
21. Q. H. ZHAO, J. M. ANDERSON, A. HILTNER, G. A. LODOEN and C. R. PAYET, *J. Biomed. Mater. Res.* **26** (1992) 1019.
22. L. EMANUELSSON, L. E. ERICSON and P. THOMSEN, in Transactions World Congress of Biomaterials, Berlin, 1992, p. 355.

*Received 10 August 1993
and accepted 31 March 1994*